Measuring Properties of Point Defects by Electron Microscopy: The Ga Vacancy in GaAs

J-L. Rouviere,[a] Y. Kim, J. Cunningham, J. A. Rentschler, A. Bourret,[a] and A. Ourmazd[b]

AT&T Bell Laboratories, Holmdel, New Jersey 07733

Exploiting the high spatial resolution and sensitivity of chemical mapping, we measure the intermixing in a series of microscopic marker layers imbedded in GaAs to detect the passage of Ga vacancies injected at the surface before the steady state has been reached. We thus deduce each of the formation and migration enthalpies for the Ga vacancy under technologically relevant conditions. More generally, we show how multilayers may be used as microscopic laboratories to investigate the properties of intrinsic point defects in solids.

Scientifically, intrinsic point defects are the elementary excitations of a solid. Technologically, they play a crucial role in controlling solid-state processes. Accurate measurement of the formation (H_f) and migration (H_m) enthalpies for intrinsic point defects is thus of scientific and technological significance. For good experimental reasons, one has often to contend with a scientifically incomplete and technologically inadequate description of a defect in terms of its total "activation enthalpy" $Q = H_f + H_m$. Extensive experimental work on GaAs has produced a generally accepted value for the diffusion activation enthalpy of the Ga vacancy (V_{Ga}) [1]. Sophisticated theoretical calculations have yielded only the formation enthalpies H_f for point defects in GaAs [2–4]. Thus, comparison between results from experiment (giving $H_f + H_m$) and theory (giving H_f) has not been possible.

In this Letter, we outline a microscopic technique for measuring separately the fundamental parameters that control intrinsic defect formation and migration, and demonstrate its practicality by presenting results for the V_{Ga} in GaAs. We also show how complex doping profiles may be used to distinguish between competing mechanisms for impurity-enhanced interdiffusion [1,5,6]. Conceptually, our approach is not new. We inject a selected point defect type (in this case V_{Ga} into GaAs) by annealing in an appropriate ambient [7], and detect the arrival and passage of the defects by monitoring the broadening of a series of marker layers imbedded in the sample. What is new is that we employ highly sensitive microscopic techniques [8,9] to measure atomic-scale changes in the marker layers long before the steady state is reached, and thus extract the formation and migration energies separately.

To appreciate the principle of our experiment, consider the diffusion of V_{Ga} introduced at the surface [7] through a homogeneous sample containing a series of ideal marker layers [10]. The passage of the defects causes intermixing between the marker and host atoms, with a coefficient

$$D = c_v(z,t,T)d_{0v}e^{-H_m/kT}. \tag{1}$$

c_v is the intrinsic defect (in our case V_{Ga}) concentration at depth z, time t, and temperature T, d_{0v} is a preexponential factor, and the other symbols have their usual meanings. When vacancies are injected from the surface

into a sample containing an initially uniform vacancy concentration c_i, the concentration at (z,t,T) can be immediately written down as [11]

$$c_v(z,t,T) = (c_s - c_i)\mathrm{erfc}(z/2L_v) + c_i. \tag{2}$$

$c_s = c_0 e^{-(H_f - TS_f)/kT}$ is the near-surface (equilibrium) vacancy concentration, S_f is the formation entropy, c_0 depends on the ambient, doping, and temperature [1], and $L_v = (d_v t)^{1/2} = (d_{0v}t)^{1/2}e^{-H_m/2kT}$ is the vacancy diffusion length. Substituting for c_v in Eq. (1), the interdiffusion coefficient at a marker layer at (z,t,T) is given by

$$D(z,t,T) = d_{0v}e^{-H_m/kT}(c_0 e^{-(H_f - TS_f)/kT} - c_i)$$

$$\times \mathrm{erfc}\left(\frac{ze^{H_m/2kT}}{2(d_{0v}t)^{1/2}}\right) + d_{0v}e^{-H_m/kT}c_i. \tag{3}$$

The first term describes the intermixing caused by the vacancies arriving from the surface; the second, the intermixing due to the vacancies already present in the bulk before any injection from the surface. The experimental observable is the total intermixing at each marker layer, given by $\Delta L^2 = L^2 - L_0^2 = \int_0^{t_{anneal}} D(z,t,T)dt$, where L_0 is the initial width of the interface between the matrix and the marker layer. As a result of a lack of sensitivity and spatial resolution, experiments are generally conducted in the "steady-state" regime, where $\mathrm{erfc} \approx 1$ and $c_s \gg c_i$. Under such conditions, Eq. (3) reduces to

$$D(T) = d_{0v}e^{S_f/k}c_0 e^{-Q/kT}. \tag{4}$$

Measurements in the steady-state regime, therefore, yield only the total activation energy Q. We measure D versus depth z and temperature T *before* the steady state has been reached, when the full expression given in Eq. (3) is operative. This yields each of the activation, formation, and migration enthalpies Q, H_f, and H_m *separately*. Measuring the small amounts of marker matrix intermixing that occur during approach to steady state requires high spatial resolution and chemical sensitivity. We use chemical mapping, a quantitative electron microscopic technique [8,9,12], capable of measuring interdiffusion coefficients as small as 10^{-22} cm^2/s at individual interfaces.

We now describe how a judicious choice of marker layers, combined with the high spatial resolution of chemical

mapping, allows us to determine whether impurity-enhanced intermixing [5] is controlled by the position of the Fermi level alone [1,5], or is due to pairing with dopants [6]. As markers, we use twenty 50-Å-thick $Al_{0.4}Ga_{0.6}As$ layers, separated by 100-Å-thick GaAs quantum wells (Fig. 1). The activation energy for group-III atomic diffusion changes by less than 200 meV as the composition is changed from GaAs to $Al_{0.4}Ga_{0.6}As$ [13]. This is less than $3kT$ at the diffusion temperatures we use (~600°C), making $Al_{0.4}Ga_{0.6}As$ a near-ideal marker (see also below). We place dopants (10^{18} Si/cm^3) only in one-half of the GaAs quantum wells [14]. Self-consistent calculations [15] show that in this structure, 5×10^{17} cm^{-2} carriers are present in the GaAs wells, and the band bending is < 10 meV (which is $\ll kT$ at 600°C) (Fig. 1). This sample structure thus places dopants at only one interface of each $Al_{0.4}Ga_{0.6}As$ marker layer, while providing the same carrier concentration at both. By comparing the intermixing at the two interfaces, we are able to immediately determine whether V_{Ga} diffusion is affected by the presence of dopant atoms or the position of the Fermi level, and thus distinguish between defect-pairing and Fermi-level models.

The final "twist" in our approach involves the choice of the layer capping the multiquantum well structure. In one set of samples (set A), the $Al_{0.4}Ga_{0.6}As$/GaAs multilayer was capped with a 50-Å-thick GaAs layer, doped to 10^{18} Si/cm^3. This served two purposes. First, it screened near-surface electric fields due to Fermi-level pinning, etc. Second, by increasing the surface concentration of V_{Ga} [1,5], it acted as a defect filter, promoting the formation and injection of V_{Ga} at rather low temperatures (~600°C). In the second set of samples (set B), the multilayer was buried beneath a 6000-Å-thick, undoped GaAs cap to reduce defect creation at the surface, and prevent the defects created at the surface from reaching the multilayer. In this way, we were able to directly determine the contribution of the point defects frozen in the sample during growth, i.e., to measure the second

term in Eq. (3).

In detail, our experiments were carried out as follows. The multilayers were grown at 600°C by molecular-beam epitaxy. Bulk samples were annealed for 2 h at 600–650°C in 2.5-ml, evacuated (~5×10^{-8} Torr), sealed quartz ampoules, containing 3 mg of As. At the annealing temperatures used, this sets an As_4 partial pressure of ~0.24 atm, with no solid As residue. As-grown and annealed samples were mechanically polished in ⟨100⟩ cross section, and chemically etched to perforation; quantitative chemical maps were obtained by a JEOL 4000EX high-resolution transmission electron microscope, operating at 400 kV. Chemical mapping is able to detect single Ga→ Al changes in each atomic column [9], reveal the composition profile across individual interfaces with atomic plane resolution [12,16] (Fig. 2), and directly reveal the presence of nonlinearities in the diffusion process [12]. No such nonlinearities were observed, confirming the near ideality of $Al_{0.4}Ga_{0.6}As$ as a marker. Using the unannealed profile for each interface as the initial boundary condition, the linear diffusion equation was solved to fit the annealed profile, and deduce the intermixing ΔL^2 at each interface of each marker layer.

We now describe our results. The intermixing is the same at adjacent interfaces 50 Å apart, only one of which

FIG. 2. (a) Chemical lattice image of an $Al_{0.4}Ga_{0.6}As$/GaAs marker/matrix interface before annealing. The compositional information is encoded in the local patterns that form the image. This information is quantitatively extracted by a pattern recognition approach, to determine the composition of each atomic column in the image. (b) Marker/matrix composition profiles before and after annealing at 650°C for 2 h. Each point gives the composition of a ~100-Å segment of an atomic plane. The error bars are smaller than the dots. The solid and dotted lines are solutions of the linear diffusion equation.
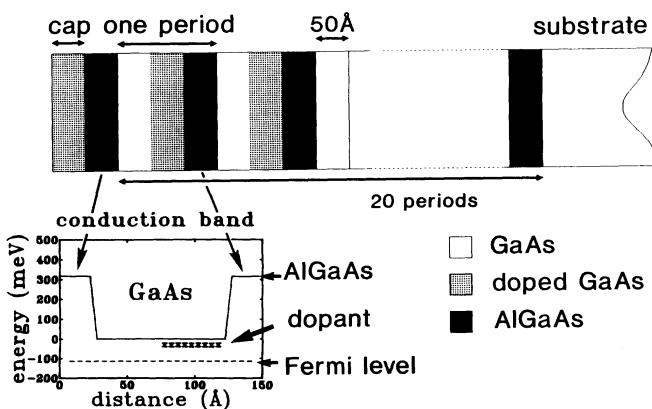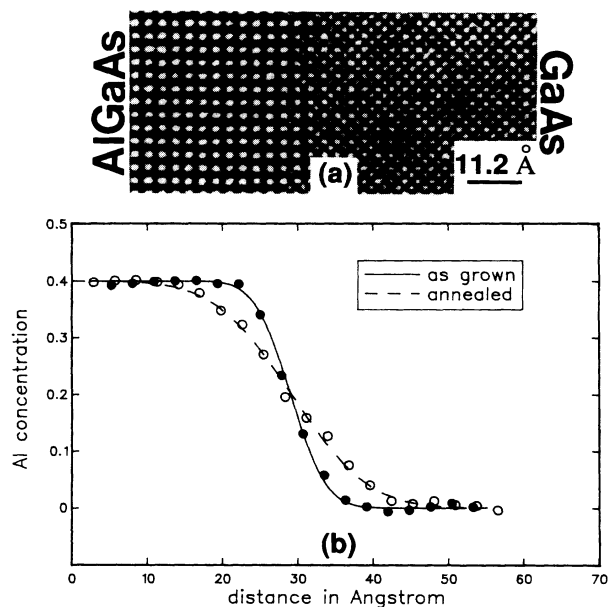
FIG. 1. Schematic diagram of multilayers used. The cap layer was either heavily doped, 50-Å-thick, or undoped, 6000-Å-thick GaAs. Inset: Result of self-consistent calculation of band bending and Fermi-level position at 600°C.

is in the immediate proximity of dopant atoms. In agreement with Deppe and Holonyak [5] and Tan, Gösele, and Yu [1], this clearly establishes that the position of the Fermi level (which is the same at both interfaces), and not the physical presence of dopant atoms, gives rise to impurity-enhanced intermixing. We thus base the subsequent analysis on the (observed cubic) dependence of the interdiffusion coefficient on the free carrier concentration [1]. Turning to the measurement of Q, H_f, and H_m for the V_{Ga}, Fig. 3 shows the intermixing $\Delta L^2/t_{anneal}$ after annealing samples from set A at three different temperatures and samples from set B at one temperature. (The thin, heavily doped cap layer in set A causes strong V_{Ga} injection from the surface; the thick, undoped cap in set B prevents injection into the multilayer.) These data were simultaneously fitted by the expression

$$D(z,t,T) = P_{As_4}^{1/4} \left[\frac{n_d}{n_i(T)} \right]^3 D_0 e^{-Q/kT} \text{erfc}(\Lambda)$$
$$+ d_{0r} e^{-H_m/kT} \text{erf}(\Lambda) c_i , \tag{5}$$

which explicitly states the doping and pressure dependence of the preexponential factor in Eq. (3). Here $D_0 = d_{0r} c_0 (n_i/n_d)^3 P_{As_4}^{-1/4} e^{S_f/k}$, n_i and n_d are intrinsic carrier and dopant concentrations [1], and $\Lambda = z e^{H_m/2kT} / 2(d_{0r}t)^{1/2}$. Q, H_m, c_i, and d_{0r} were used as free parameters for the fits [17]. The preexponential factor D_0 was taken from Tan, Gösele, and Yu [1], where it was deduced from a large compilation of data over an extended temperature range. The best simultaneous fit, represented by the solid lines in Fig. 2, has a goodness of fit of 0.997. The values deduced for the various thermodynamic parameters are summarized in Table I. Uncertainties in the deduced parameters were estimated by a Monte Carlo procedure, allowing D_0 to vary by up to 2 orders of
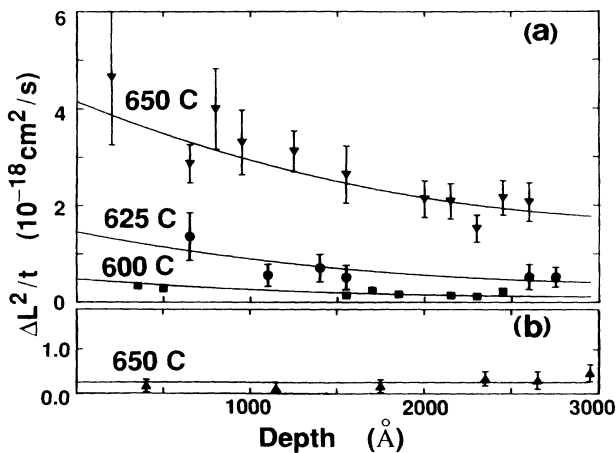

FIG. 3. Plot of $\Delta L^2/t_{expt}$ vs depth of marker layer. (a) Multilayer capped by a heavily doped, 50-Å-thick GaAs layer, causing strong injection of V_{Ga} into the multilayer. (b) Multilayer buried under an undoped, 6000-Å-thick GaAs cap, to prevent significant V_{Ga} injection into the multilayer.

magnitude. Allowing D_0 to vary freely increases the uncertainties (e.g., from 0.2 to 0.7 and from 0.5 to 0.9 eV for Q and H_f, respectively), but leaves the deduced parameters within the uncertainties quoted in Table I.

We now place these results in context. The activation enthalpy we deduce (5.7 ± 0.2 eV) is in excellent agreement with the generally accepted value (6 eV) [1,18]. The value of 4.0 ± 0.5 eV for H_f is in good agreement with the calculations of Scheffler and Dabrowski [3], which predict $H_f \geq 3.5$ eV under our experimental conditions ($P_{As_4} = 0.24$ atm; Fermi level 0.12 eV below the conduction band). It is difficult to extract H_f for these conditions from the work of Zhang and Northrup [4], but there appears to be general agreement between our measurements and their calculated value for H_f (4 eV in the As-rich limit; Fermi level at the conduction band). Our value for the formation entropy [19] [(32.9 ± 5)k_B] is large, but close to the estimate by Tan, Gössele, and Yu [1] for the total activation entropy ($\sim 25k_B$). We note that at 600 °C, the entropy term (2.5 eV) is a substantial fraction of the formation enthalpy. This points to the importance of the entropy term in diffusion in the GaAs system, and the need for caution in using absolute-zero calculations for predictive purposes.

We now list the more general implications of our work. First, our experiments measure the properties of $\sim 10^{16} \times V_{Ga}/cm^3$ (c_i in Table I), sampling regions $\sim 10^{-16}$ cm^3 in volume. Thus, on average, the sampling volume contains only one vacancy at any time during the anneal. This "average" vacancy crosses the marker interface many times during the anneal, causing an intermixing easily detectable by our technique [Fig. 3(b)]. Thus, in contrast to the very high defect concentrations required to detect point defects by traditional microscopic techniques [20], we have demonstrated a microscopic method for measuring the properties of realistic concentrations of point defects. Second, the parameters we have measured for the formation and migration of the V_{Ga} can be directly used for technologically relevant predictive purposes, for example, in process simulation. Third, our results have established a link between theory and experiment, indicating the success and shortcomings of state-of-the-art calculations. Finally, we have demonstrated that the

TABLE I. Thermodynamic properties of V_{Ga} in GaAs (referred to the intrinsic material at $P_{As_4} = 1$ atm).

Parameter	Symbol (unit)	Value
Activation enthalpy	Q (eV)	5.7 ± 0.2
Formation enthalpy	H_f (eV)	4.0 ± 0.5
Migration enthalpy	H_m (eV)	1.7 ± 0.5
Formation entropy	S_f (k_B)	32.9 ± 5
Migration preexponential factor	d_{0r} (cm^2/s)	3.9×10^{-4}
"Grown-in" V_{Ga} concentration[a]	c_i (cm^{-3})	1.2×10^{16}
Equilib. V_{Ga} concentration[a]	c_s (cm^{-3})	7.2×10^{16}

[a] n type, 5×10^{17} electrons/cm^3, 600 °C.

extreme sensitivity and spatial resolution of chemical mapping allow multilayers to be used as microscopic laboratories to investigate point defect reactions in solids.

In conclusion, we have outlined a microscopic technique for measuring the fundamental parameters that control intrinsic point defect formation and migration, and demonstrated its practicality by presenting results for the V_{Ga} in GaAs.

[a]Permanent address: Departement de Recherche Fondamental, Centre d'Etudes Nucléaires de Grenoble 85X, 38041, Grenoble CEDEX, France.

[b]To whom correspondence should be addressed.

[1] For an excellent review, see T. Y. Tan, U. Gösele, and S. Yu, Crit. Rev. Solid State Mater. Sci. 17, 47 (1991).

[2] G. A. Baraff and M. Schlüter, Phys. Rev. Lett. 55, 1327 (1985).

[3] M. Scheffler and J. Dabrowski, Philos. Mag. A 58, 107 (1988).

[4] S. B. Zhang and J. E. Northrup, Phys. Rev. Lett. 67, 2339 (1991).

[5] For an excellent review, see D. G. Deppe and N. Holonyak, Jr., J. Appl. Phys. 64, R93 (1988).

[6] J. A. Van Vechten and U. Schmidt, J. Vac. Sci. Technol. B 7, 827 (1989).

[7] Annealing in an As-rich ambient injects V_{Ga} and As interstitials. It has been shown [5] that each defect type causes intermixing on its own sublattice. By monitoring Ga/Al intermixing, we measure the properties of the V_{Ga} only.

[8] A. Ourmazd, D. W. Taylor, J. Cunningham, and C. W. Tu, Phys. Rev. Lett. 62, 933 (1989).

[9] A. Ourmazd, F. H. Baumann, M. Bode, and Y. Kim, Ultramicroscopy 34, 237 (1990).

[10] Our arguments apply to vacancies and to interstitials diffusing by the "kick out" mechanism [1].

[11] See, e.g., J. Crank, Mathematics of Diffusion (Oxford Univ. Press, New York, 1989).

[12] Y. Kim, A. Ourmazd, M. Bode, and R. D. Feldman, Phys. Rev. Lett. 63, 636 (1989).

[13] L. L. Chang and A. Koma, Appl. Phys. Lett. 29, 138 (1976).

[14] Measured diffusion coefficient of Si in GaAs [J. J. Harris, J. B. Clegg, R. B. Beall, J. Castagne, K. Woodbridge, and C. Roberts, J. Cryst. Growth 111, 239 (1991)] indicate that during our anneals, the Si dopants move by ≤ 5 Å.

[15] G. Livescu, D. A. B. Miller, D. S. Chemla, M. Ramaswamy, T. Y. Chang, N. Sauer, A. C. Gossard, and J. H. English, IEEE J. Quantum Electron. 24, 1677 (1988).

[16] M. Bode, A. Ourmazd, J. Cunningham, and M. Hong, Phys. Rev. Lett. 67, 843 (1991).

[17] The presence of the undoped-buffer-layer/substrate produces a small correction, easily incorporated by a solution consisting of a sum of error functions. This modified expression was used to obtain the fits shown.

[18] There have been two previous attempts to measure H_f and H_m: S. Y. Chiang and G. L. Pearson, J. Appl. Phys. 46, 2986 (1975); K. B. Kahen, D. L. Peterson, G. Rajeswaran, and D. J. Lawrence, Appl. Phys. Lett. 55, 651 (1989). The results of Chiang and Pearson are at variance with modern diffusion data. The measurements of Kahen et al. suffered from experimental difficulties in establishing reproducible surface boundary conditions. We therefore refrain from discussing these results.

[19] The formation entropy S_f is deduced as follows: $c_0 = (P_{As}/135.1 T^{5/2})^{1/4}(n_d/n_i)^3$ [1]. Thus, $S_f = k \ln[(135.1 \times T^{5/2})^{1/4}D_0/d_0]$.

[20] J. M. Gibson and M. L. MacDonald, in Characterization of Defects in Materials, edited by R. W. Siegel, R. Sinclair, and J. R. Weertman, MRS Symposia Proceedings No. 82 (Materials Research Society, Pittsburgh, 1987), p. 109.
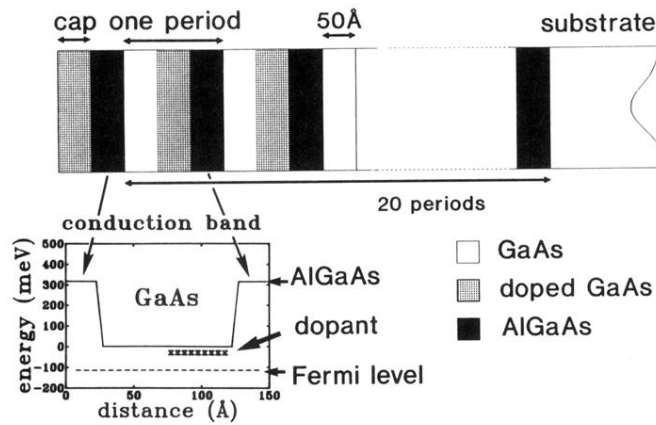
FIG. 1. Schematic diagram of multilayers used. The cap layer was either heavily doped, 50-Å-thick, or undoped, 6000-Å-thick GaAs. Inset: Result of self-consistent calculation of band bending and Fermi-level position at 600 °C.
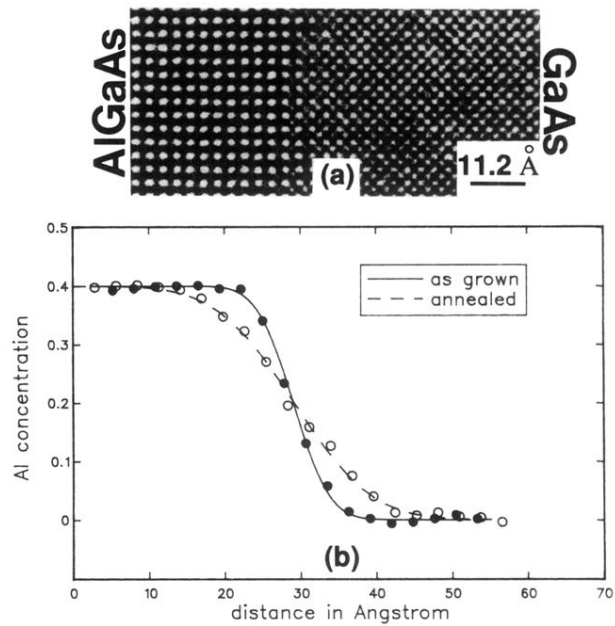
FIG. 2. (a) Chemical lattice image of an $Al_{0.4}Ga_{0.6}As/GaAs$ marker/matrix interface before annealing. The compositional information is encoded in the local patterns that form the image. This information is quantitatively extracted by a pattern recognition approach, to determine the composition of each atomic column in the image. (b) Marker/matrix composition profiles before and after annealing at 650 °C for 2 h. Each point gives the composition of a ~100-Å segment of an atomic plane. The error bars are smaller than the dots. The solid and dotted lines are solutions of the linear diffusion equation.